



NLR-TP-2001-055

## **Distortion of conformal antennas on aircraft structures**

H. Schippers, H. van Tongeren, J. Verpoorte  
and G. Vos



NLR-TP-2001-055

## **Distortion of conformal antennas on aircraft structures**

H. Schippers, H. van Tongeren, J. Verpoorte  
and G. Vos

This investigation has been carried out partly under a contract awarded by the Scientific Research Division of the Directorate of Materiel of the Royal Netherlands Air Force, contract number N98/10.

The Scientific Research Division of the Directorate of Materiel of the Royal Netherlands Air Force has granted NLR permission to publish this report.

This report is based on a presentation held at the SPIE's 8<sup>th</sup> annual international Symposium on Smart Structures and Materials, Newport Beach, California (USA), 4-8 March 2001.

The contents of this report may be cited on condition that full credit is given to NLR and the authors.

Division:	Avionics
Issued:	7 February 2001
Classification of title:	Unclassified



## Contents

<b>ABSTRACT</b>	3
<b>1. INTRODUCTION</b>	3
<b>2. CALCULATION OF DEFORMATION OF ANTENNA SURFACE</b>	4
2.1 Elasto-mechanical modelling	4
2.2 Aerodynamic analysis	5
2.3 Computation of dynamic deformations	5
2.4 Unsteady high frequency aerodynamics	6
<b>3. PHASED ARRAY ON RECONNAISSANCE POD</b>	8
3.1 Vibration modes	8
3.2 Frequency response analysis	8
<b>4. ELECTRO-MAGNETIC MODELLING</b>	9
<b>5. DISTORTION OF A SIDE-LOOKING AIRBORNE RADAR ANTENNA</b>	10
<b>6. CONCLUSIONS</b>	10
<b>REFERENCES</b>	11

12 Figures

(14 pages in total)



## **Distortion of Conformal Antennas on Aircraft Structures**

Harmen Schippers, Hans van Tongeren, Jaco Verpoorte and Guus Vos  
National Aerospace Laboratory NLR, P.O. Box 90502, 1006 BM Amsterdam,  
The Netherlands

### **ABSTRACT**

Conformal antennas on aircraft allow the use of non-conventional antenna locations such as the skin of the aircraft. However, when antennas are installed at these locations they are subject to steady and unsteady aerodynamic loads. The inertial forces and these aerodynamic loads will cause deformations and vibrations of the total antenna surface. The effect of these distortions on antenna performance will be most significant on highly directional antennas. The aim of the present paper is to describe technology development for estimating the effects of surface distortion on antenna performance. The technology is applied to a Side-Looking Airborne Radar (SLAR) antenna on a reconnaissance pod mounted on a fighter type aircraft. This generic SLAR antenna is a phased array antenna covering two faces of the pod: one part on the vertical side face and one part on the lower face of the pod. Radiation patterns are computed for distorted antenna surfaces. The computational model for the determination of the disturbed radiation pattern is based on geometrical parameterisation of the Stratton-Chu integral equations.

**Keywords:** Conformal antennas, deformation, radiation pattern.

### **1. INTRODUCTION**

The use of conformal antennas on aircraft allows the choice of non-conventional antenna locations such as the skin of the aircraft. The inertial forces and the aerodynamic loads will cause deformations and vibrations of the total antenna surface. The effect of these deformations and vibrations on the antenna performance will be most significant on highly directional antennas. In order to assess the effects of surface vibrations and deformations on the performance of conformal antennas on aircraft, NLR carries out a National Technology project (under contract of the Netherlands Ministry of Defence) with the title: Conformal Load-bearing Antennas on Aircraft Structures (acronym CLAAS). This technology development requires contributions from the following research disciplines: 1. Aerodynamics research, 2. Aero-elastic research, 3. Structural dynamic research and 4. Avionics research. The Aerodynamics research provides knowledge about the size of steady and unsteady aerodynamic loads at the antenna locations. The Aero-elastics research provides knowledge about amplitudes and frequencies of vibrations of the antenna surface and the surrounding aircraft structure due to unsteady aerodynamic loads. The Structural dynamic research provides knowledge about the eigenfrequencies and vibration modes of the unloaded aircraft structure (at locations of the antenna locations) and provides knowledge about the magnitude of local steady displacements (due to steady aerodynamic loads). The Avionics research provides knowledge about operational functions of conformal antennas, knowledge about requirements on possible antenna locations, knowledge about the modelling of conformal antennas and knowledge about effects



of vibrations on performance of conformal antennas. An overview of the computational modelling process is presented in Figure 1. The process involves the specification of aircraft and antenna data, steady and unsteady aerodynamic calculations as well as electromagnetic analysis of perturbed antenna surfaces. The aim of the present paper is to describe the technology development and to apply the technology to a Side-Looking Airborne Radar (SLAR) antenna on a reconnaissance pod mounted on a fighter type aircraft (see Figure 2). This generic SLAR antenna is characterized by phased array antennas on two surfaces of the pod: one on the vertical side face of the pod and one on the lower face of the pod. The antennas on one side face and on the lower face are used to design a side-looking airborne radar antenna in a prescribed direction. The vibration modes of the front part of an unloaded reconnaissance pod have been computed. This knowledge is used to prescribe the distortion of the antenna surface. The effects of distortion on the radiation pattern are investigated. The computational model for the determination of the disturbed radiation pattern is based on geometrical parameterisation of the Stratton-Chu integral equations.

## 2. CALCULATION OF DEFORMATION OF ANTENNA SURFACE

Through the years the analysis of the dynamics of aircraft has been based on separate calculation of vibration characteristics of the aircraft structure and unsteady airloads. The vibration modes and reduced frequencies are computed by means of elasto-mechanical modelling. The unsteady airloads are then calculated for a range of reduced frequencies and vibration modes by unsteady aerodynamic analysis methods. Subsequently, the deformation of the aircraft structure (i.e. the amplitudes) is computed by combining the vibration modes and the unsteady airloads for representative flight conditions (e.g. a gust input). The generalised modal deflection system of the aircraft structure relates the amplitudes of the vibration modes to the unsteady dynamic loads. This approach implies that only the relevant flexible vibration modes have to be incorporated in the calculation of the deformation of the aircraft structure. An overview of the computational process for the calculation of deformation of the antenna surface is displayed in Figure 3.

### 2.1 Elasto-mechanical modelling

As a representative test case the vibration characteristics of a fighter aircraft are discussed. The elasto-mechanical calculations require the availability of structural finite element data of the aircraft as well as computational methods. For the aircraft the vibration modes are distinguished for global modes (related to low frequency oscillations) and local modes (related to high frequency oscillations). For low frequency oscillations the deformation of the aircraft structure is mainly governed by global vibration modes. In this case the displacement of the panel of the conformal antenna is nearly rigid and the mutual positions of the patches of the antenna do not change. On the other hand, for high frequency oscillations the deformation of part of the aircraft structure (e.g. the location of the conformal antenna) is mainly described by local vibration modes. In this case the panel is subject to a flexible motion and the mutual positions of the patches will change during a cycle of oscillation.



For the computation of the global vibration modes a structural model is required of the relevant part of the aircraft (e.g. fuselage, wing or vertical tail), where many details of the structure are not taken into account. However, for the computation of local vibration modes a more detailed model is required for a part of the aircraft structure where the antenna will be located. In this case, the finite element model should at least include the mass and stiffness properties of the spars, stiffeners and the skin plate.

## 2.2 Aerodynamic analysis

The prediction of airloads on oscillating aircraft structures in subsonic and transonic flow requires the application of unsteady aerodynamic computational methods. Such methods are being developed since the seventies. For relatively low frequency oscillations, global unsteady airloads can be computed by means of so-called doublet lattice methods (these methods assume that the unsteady aerodynamic disturbances are small relative due to the steady aerodynamic flow state of a stationary aircraft). For relatively high frequency oscillations, local unsteady airloads can be calculated by means of so-called piston theory. This theory is based on a local relation (i.e. locally at the antenna surface) between pressure and normal component of the fluid velocity. A computational method based on piston theory is developed in the framework of the CLAAS project. The aero-elastic analysis requires that the static and dynamic deformations of the aircraft geometry are determined, subject to aerodynamic and external forces acting on the aircraft. The geometrical state of the aircraft can be described by the superposition of:

- the jig shape (i.e. the shape of the aircraft in unloaded state),
- the deformation due to steady aerodynamic forces (i.e. the change from the jig shape to the design shape under cruise conditions) and
- the dynamic deformations which are related to displacements belonging to some prescribed vibration modes.

The amplitudes of the external forces are usually prescribed in relation to representative flight conditions.

## 2.3 Computation of dynamic deformations

The part of the aircraft containing the conformal antenna is denoted by the boundary surface  $S$ . It is assumed that the dynamic deformations are deviations from a steady state. It is assumed that the dynamic deformations can be described by a linear combination of a selected set of vibration modes, which are denoted by  $\vec{\phi}_\nu$ ,  $\nu = 1, \dots, N$ . The dynamic displacement  $\vec{d}$  can then be approximated by

$$\vec{d} = \sum_{\nu=1}^N q_\nu \vec{\phi}_\nu \quad (1)$$

The coefficients  $q_\nu$  are known as the generalized co-ordinates of the vibration modes. The values of  $q_\nu$  follow from the solution of the generalized modal deflection system which reads

$$M \frac{d^2 \vec{q}}{dt^2} + D \frac{d\vec{q}}{dt} + K\vec{q} = \vec{F}^a + \vec{F}^e \quad (2)$$

The matrices  $M$ ,  $D$  and  $K$  are the generalized mass, damping and stiffness matrices, which result from the elasto-mechanical modelling. These matrices are related to the selected set of vibration modes. Furthermore,  $\vec{F}^a$  denotes the



generalized aerodynamic force and  $\vec{F}^e$  denotes a prescribed external force, which is typical for representative flight conditions. The basis of vibration modes  $\vec{\phi}_i$  can be defined by a set of global or by a set of local vibration modes. The actual choice depends on the relevant part of the aircraft surface to be analyzed. Assume that  $\vec{d}$  varies in time harmonically with angular frequency  $\omega$ . Then, equation (2) can be written as:

$$(K + j\omega D - \omega^2 M)\vec{q} = \vec{F}^a + \vec{F}^e . \quad (3)$$

Here the components of the generalized aerodynamic force  $\vec{F}^a$  are given by

$$F_i^a = -\frac{1}{2}\rho_\infty U_\infty^2 \int_S C_p \vec{\phi}_i \cdot \hat{n} dS , \quad (4)$$

with  $\hat{n}$  the unit outward normal vector to  $S$ . Furthermore  $\rho_\infty$  and  $U_\infty$  are the air density of the undisturbed flow and the airspeed, respectively. The pressure coefficient  $C_p$  is given by

$$C_p = \frac{p - p_\infty}{\frac{1}{2}\rho_\infty U_\infty^2} , \quad (5)$$

where  $p$  is the unsteady pressure. For relatively low frequency oscillations, the unsteady pressure can be computed by means of so-called doublet lattice methods, which are available in the structural analysis software package NASTRAN. However, for relatively high frequency oscillations  $p$  can be approximated by means of piston theory.

#### 2.4 Unsteady high frequency aerodynamics

In piston theory the pressure difference  $p - p_\infty$  is approximated by

$$p - p_\infty = \rho_\infty a_\infty w , , \quad (6)$$

with  $w$  the normal velocity of the dynamic displacement of the boundary surface  $S$ . Substitution of (6) into (5) yields

$$C_p = \frac{p - p_\infty}{\frac{1}{2}\rho_\infty U_\infty^2} = \frac{2}{M_\infty} \frac{w}{U_\infty} \quad (7)$$

The normal velocity  $w$  follows from the total derivative of the normal dynamic displacement with respect to time ,i.e.

$$w = \frac{d(\hat{n} \cdot \vec{d})}{dt} = \frac{\partial(\hat{n} \cdot \vec{d})}{\partial t} + U_\infty \frac{\partial(\hat{n} \cdot \vec{d})}{\partial x} , \quad (8)$$

with  $\vec{d}$  given by equation (1). Since  $\vec{d}$  varies in time harmonically with  $\omega$ , equation (8) can be written as

$$w = j\omega \hat{n} \cdot \vec{d} + U_\infty \frac{\partial(\hat{n} \cdot \vec{d})}{\partial x} \quad (9)$$

Substitute this relation into (7) to obtain

$$C_p = \frac{2}{M_\infty} \left( \frac{j\omega}{U_\infty} \hat{n} \cdot \vec{d} + \frac{\partial(\hat{n} \cdot \vec{d})}{\partial x} \right) \quad (10)$$



Next substitute (1) into (10) to obtain the pressure coefficient for vibration mode  $v$ , i.e.

$$C_{p,v} = \frac{2}{M_\infty} \left( j\omega \frac{\hat{n} \cdot \vec{\phi}_v}{U_\infty} + \frac{\partial(\hat{n} \cdot \vec{\phi}_v)}{\partial x} \right) \quad (11)$$

Then the  $i^{\text{th}}$  component of the generalized aerodynamic force  $\vec{F}^a$  becomes

$$F_i^a = -\frac{1}{2} \rho_\infty U_\infty^2 \int \sum_{S,v=1}^N q_v C_{p,v} \vec{\phi}_i \cdot \hat{n} dS. \quad (12)$$

Substitute (11) into (12) and define

$$A_{i,v} = A(\vec{\phi}_i, \vec{\phi}_v) = -\frac{1}{2} \rho_\infty U_\infty^2 \int_S \hat{n} \cdot \vec{\phi}_i \frac{2}{M_\infty} \left( j\omega \frac{\hat{n} \cdot \vec{\phi}_v}{U_\infty} + \frac{\partial(\hat{n} \cdot \vec{\phi}_v)}{\partial x} \right) dS. \quad (13)$$

Then,  $F_i^a$  becomes

$$F_i^a = \sum_{v=1}^N A_{i,v} q_v \quad (14)$$

Inspection of (13) reveals that the first term of the integral yields a contribution to the damping matrix, while the second term yields a contribution to the stiffness matrix. As a consequence, the unsteady aerodynamic force can be written as

$$\vec{F}^a = Q^a \vec{q}, \quad (15)$$

with  $Q^a = (K^a + j\omega D^a)$ .

The external excitation may be due to atmospheric turbulence or due to control surface movements. In this paper, the external force is given by

$$\vec{F}^e = Q^g(\omega) \vec{q}^g, \quad (16)$$

with  $\vec{q}^g$  the generalised co-ordinates related to the turbulence motion. The matrix  $Q^g$  is defined by

$$Q^g(\omega) = 2 \frac{\rho_\infty U_\infty}{M_\infty} w_g \int_S e^{j\omega x / U_\infty} (\hat{n} \cdot \hat{e}_z) (\hat{n} \cdot \vec{\phi}_v) dS, \quad (17)$$

with  $w_g$  the amplitude of the gust velocity. In many scenarios the values of  $w_g$  follow from the Dryden gust spectrum.

Substitution of equations (15) and (16) into (3) yields the following equation:

$$(K - K^a + j\omega(D - D^a) - \omega^2 M) \vec{q} = Q^g(\omega) \vec{q}^g. \quad (18)$$



When the frequency  $\omega$  is prescribed and the value of  $w_g$  is known, one can compute the frequency response from (18). The above approach has been verified for a rectangular plate with air flow on both sides. In that case all terms in  $A_{i,v}$  and  $Q^g$  must be multiplied by a factor 2 since these quantities were derived for one sided air flow. The outcome of the above high frequency modelling has been compared with results of the low frequency doublet lattice unsteady aerodynamics frequency response analysis of MSC NASTRAN with prescribing a similar one dimensional gust field. The results of the Piston theory calculations and NASTRAN are presented in Figure 4. Inspection of Figure 4 reveals a fair comparison, in particular for the higher frequencies. The differences can be justified by the different mathematical models, which were used for these unsteady aerodynamics calculations. This comparison provides sufficient confidence for the application of the Piston theory to predict the local unsteady airloads at the antenna surface.

### 3. PHASED ARRAY ON RECONNAISSANCE POD

The technology of the CLAAS project will be mainly applied to a fighter type aircraft. The aerodynamic and structural finite element data of such an aircraft are available at NLR. The availability is required otherwise the above approach of computational modelling cannot be performed. When aerodynamic and structural data would be available for other platforms (e.g. other aircraft, UAV's) the technology can also be used for the analysis of conformal antennas on these platforms.

For the demonstration of the technology NLR considers a generic phased array antenna (see Figure 5) on a reconnaissance pod that is mounted under a fighter aircraft. The above technology has been applied to determine the vibration modes and responses in the frequency domain.

#### 3.1 Vibration modes

A structural finite element mesh has been used to compute the vibration modes of the front part of the unloaded reconnaissance pod. The first 10 eigenfrequencies are given in table 1. A relevant mode is displayed in Figure 6. These vibration modes are used to compute the unsteady airloads by means of Piston theory (see section 2.4).

Vibration mode	1	2	3	4	5	6	7	8	9	10
Resonance Frequency	170.98	175.09	184.63	203.11	213.03	225.57	229.62	235.77	249.02	255.04

Table 1 Eigenfrequencies of front part of reconnaissance pod

#### 3.2 Frequency response analysis

The unsteady aerodynamics model of section 2.4 has been implemented in a MathCad pilot program. This program has been used to compute the frequency response function for a vertical gust field passing the reconnaissance pod. The analysis was based on the first ten vibration modes belonging to the eigen-frequencies of table 1.

Figure 7 displays the frequency response function for the node with maximum deflection of the seventh vibration mode at 229.6 Hz. The calculations reveal a maximum deflection of 0.45 mm at this node for a gust speed amplitude of 1 m/sec. From inflight measurements on other components of the aircraft gust speed amplitudes of 3.5 to 16 m/sec have been observed. Hence, for the seventh vibration mode a maximum deflection between about 1 and 7 mm can be expected.



#### 4. ELECTRO-MAGNETIC MODELLING

The radiated electric field can be determined by the application of the Stratton-Chu integral representation formulas. The geometrical deformation of the antenna surface can be modelled in these formulas by introducing a geometrical parameterisation of the antenna surface. The boundary points of the undisturbed antenna surface  $S_0$  are assumed to be described by a map  $\Psi_0$ , which maps a square reference domain  $\Omega$  onto  $S_0$ . The boundary points of the displacement  $\vec{d}$  (see equation 1) are defined by a similar mapping. Then, the deformed antenna surface  $S_1$  can be described by

$$\vec{\Psi}_1(\vec{u}) = \vec{\Psi}_0(\vec{u}) + \vec{d}(\vec{u}) \quad (19)$$

with  $\vec{u} \in \Omega$ . In this paper the effects of deformation of the antenna surface on the radiation pattern are investigated for some representative vibration modes with prescribed amplitude. Then, the deformation  $\vec{d}$  is given by  $\vec{d}(\vec{u}) = \alpha \vec{\phi}_l(\vec{u})$ , with  $\alpha$  prescribed. Then equation (19) reads

$$\vec{\Psi}_1(\vec{u}) = \vec{\Psi}_0(\vec{u}) + \alpha \vec{\phi}_l(\vec{u}) \quad (20)$$

The surface current distribution on the phased array antenna is assumed to be given by prescribed magnetic surface currents along the edges of the radiating patches (i.e. radiating slots) as described in [1], pp. 48-50. In the far field the radiated electric field due to radiating patches on antenna surface  $S$  can be approximated by (see [2], pp. 87-88):

$$\vec{E}(\vec{r}) = -jk \frac{e^{-jkR}}{4\pi R} \int_S \vec{M}(\vec{r}') \times \hat{R} e^{jk\vec{r}' \cdot \hat{R}} ds' \quad (21)$$

where  $R$  is the distance from the origin to the observer and  $\hat{R}$  the unit direction vector from the origin to the observer. For the undisturbed antenna the surface  $S$  is given by  $S_0$ , while the perturbed antenna surface is given by  $S_1$ . Thus, the deformation of the surface of the antenna is modelled in the formula for the electric field by introducing the map  $\vec{\Psi}_1$  in the integral of equation (21). This formula assumes that the magnetic surface current  $\vec{M}$  is tangential to the surface  $S$ .

The numerical approach for the computation of the integral in equation (21) has been discussed in references [3] and [4]. The magnetic surface currents  $\vec{M}_0$  on the undisturbed surface are taken piecewise constant on the narrow slots along the radiating edges, while they are assumed to be zero elsewhere. The radiating slots are aligned in the flight direction (i.e. the  $\hat{x}$ -direction). The patches of the antenna array are assumed locally planar on the deformed surface  $S_1$ . Let  $\hat{n}$  be the normal vector at some patch and let  $\vec{a}_1, \vec{a}_2$  be a local tangential base. This local base is determined numerically by taking differences between edge points of patches on the perturbed surface using equation (20). This has been performed in such a way that  $\vec{a}_1$  corresponds approximately with the  $\hat{x}$ -direction. Then, the magnetic currents on the perturbed surface follow from  $\vec{M}_1 = M\vec{a}_1$ . Notice that  $\vec{a}_1, \vec{a}_2$  and  $\hat{n}$  depend on  $\alpha$  by equation (20). As a consequence of this approach, the integral in (21) reduces to the summation of the sub-integrals over the slots of the separate patches. Hence (21) can be rewritten as

$$\vec{E}(\vec{r}) = -jk \frac{e^{-jkR}}{4\pi R} \sum_p (\vec{M}_{1,p} \times \hat{R}) \int_{A_p} e^{jk\vec{r}' \cdot \hat{R}} ds' \quad (22)$$



with  $p$  the index for patch number  $p$ . Furthermore,  $A_p$  denotes the united area of the two radiating slots of patch number  $p$ . The phase integral in (22) can be computed in closed form by replacing the vector  $\vec{r}'$  by  $\vec{r}^* + \vec{a}_1\xi + \vec{a}_2\eta$ , with  $\vec{r}^*$  the center of the radiating slots.

## 5. DISTORTION OF A SIDE-LOOKING AIRBORNE RADAR ANTENNA

The effects of vibrations and deformations on the antenna performance were calculated for the case of a C-band Side-looking airborne radar (SLAR) antenna, designed on the surface of a reconnaissance pod. The antenna consists of a faceted two-dimensional conformal array of patch antennas. The number of antenna elements along-track was chosen higher than the number across-track because of higher beam-width requirements. Along-track, the array on the pod can be considered as a planar array. However, across-track, a conformal antenna array on the curved surface of the pod has been defined. Across-track the array consists of 23 elements conformal to the surface and the array length along-track is 30 elements. These antenna elements were designed to form a SLAR application, with beam elevation defined at  $135^\circ$  w.r.t. zenith (see Figure 9,  $\theta=0^\circ$  is towards zenith, the  $\varphi$ -plane is the horizontal plane with  $\varphi=0^\circ$  being the flight direction).

In this paper the deterioration of the antenna performance will be considered for a characteristic vibration mode. The frequency response calculation of section 3.2 showed a maximum deviation of  $\pm 0.5$  mm for a gust-input of 1 m/s at a frequency of 229.6 Hz. This frequency corresponds with the resonance frequency of vibration mode 7. Future structural research will provide a realistic value for the gust-input. For the time being a gust input of 10 m/s will be assumed. Then, the maximum amplitude of the vibration mode would increase to  $\pm 0.5$  cm. The deformation of the geometry according to this vibration mode is shown in Figure 8. For this example, the effects of vibration levels with a maximum of  $1/8$  lambda (approximately 6 mm) are shown in Figures 9 to 12. It can be concluded that for this level of vibration the radiation pattern will deteriorate. The beam-width of the antenna array will increase slightly, while the side lobe levels near the main beam have been increased significantly. With regard to the interpretation of the Figures 10, 11 and 12, they should be interpreted as snapshots of the radiation pattern of the SLAR antenna at maximum deformation for the specific vibration mode.

## 6. CONCLUSIONS

In this paper the computational modelling for predicting distortion of radiation patterns of conformal antennas on aircraft structures has been discussed. The deformation of a phased array antenna on a reconnaissance pod has been computed by means of elasto-mechanical modelling and high frequency unsteady aerodynamics for a certain gust input. The actual deflection (i.e. the amplitude of the deformation) depends on the magnitude of the vertical gust velocity, which has been estimated in this paper. Further research is required for obtaining more accurate values for the gust velocity at the frequencies of interest.

The electromagnetic computational model reveals a certain distortion of the radiation pattern, which has an adverse effect on the performance of the antenna. The CLAAS project is an ongoing project. In the near future the electromagnetic model will be validated. It is foreseen to carry out measurements for phased array antennas on generic structures, which are representative for both undisturbed and deformed aircraft structure skins. In addition the feasibility of compensation techniques has to be



considered. Once these items are adequately covered, this technology may be applied to future phased array antennas at non-conventional locations on the aircraft.

#### REFERENCES

1. I.J. Bahl and P. Bhartia, *Micro Strip Antennas*, Artech House, 1980.
2. S. Silver, *Microwave Antenna Theory and Design*, Peter Peregrinus, 1984.
3. H. Schippers and F. Klinker, *Analysis of Conformal Antennas on Aircraft Structures*, National Aerospace Laboratory NLR, TP99066, 1999.
4. J. Verpoorte, H. Schippers and G. Vos, *Technology for Conformal Load-bearing Antennas on Aircraft Structures*, National Aerospace Laboratory NLR, TP2000-520, 2000.

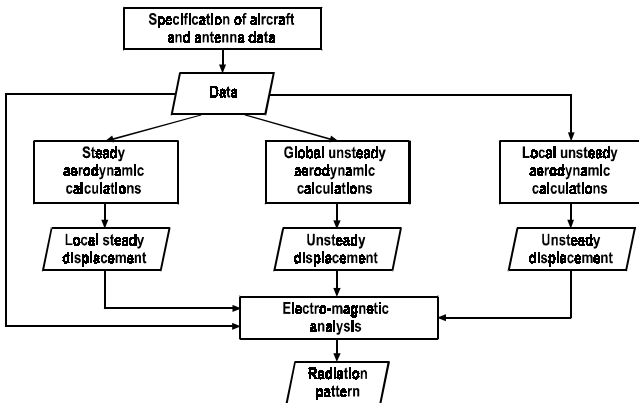


Figure 1 Overview of the computation modelling process

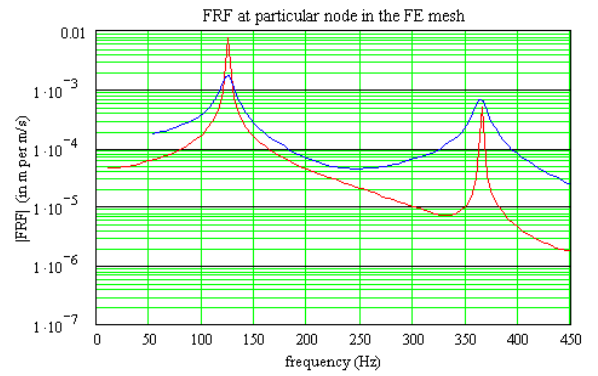


Figure 4 Frequency response function for a rectangular plate (air flow on both sides);

red curve: MSC NASTRAN (doublet lattice), blue curve: "NLR implementation of piston theory"

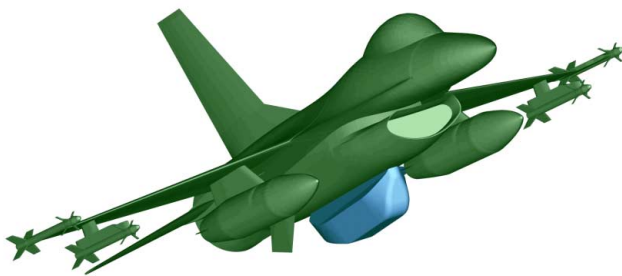


Figure 2 Fighter aircraft with reconnaissance pod

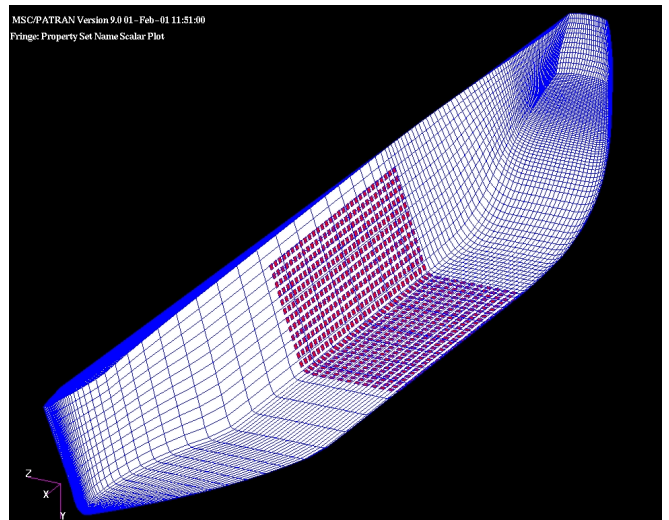


Figure 5 Phased array antenna on reconnaissance pod

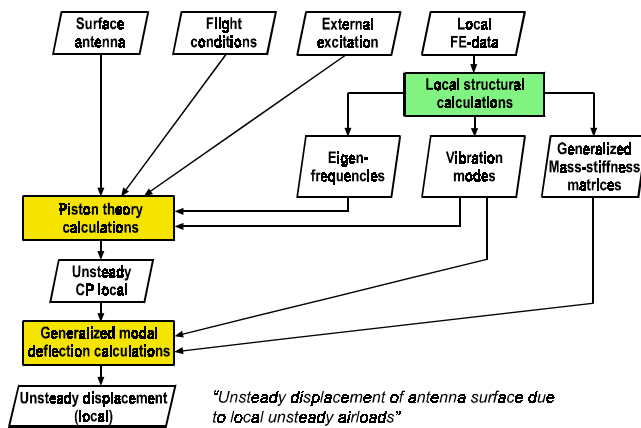


Figure 3 Computational process for prediction of displacement of antenna surface due to local unsteady airloads.

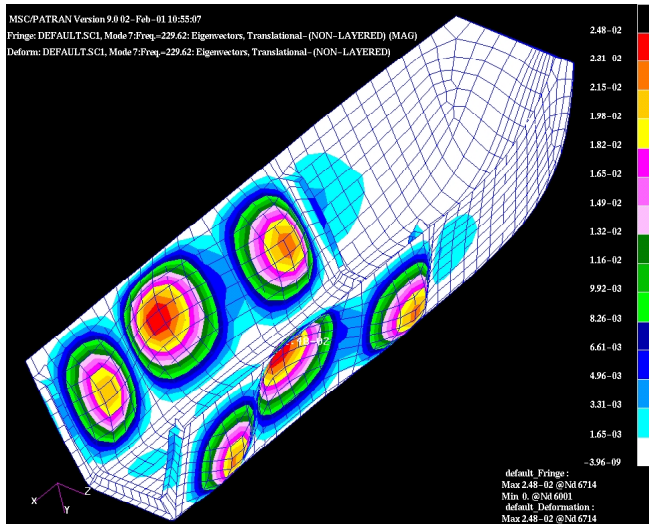


Figure 6 Vibration mode at 229.62 Hz

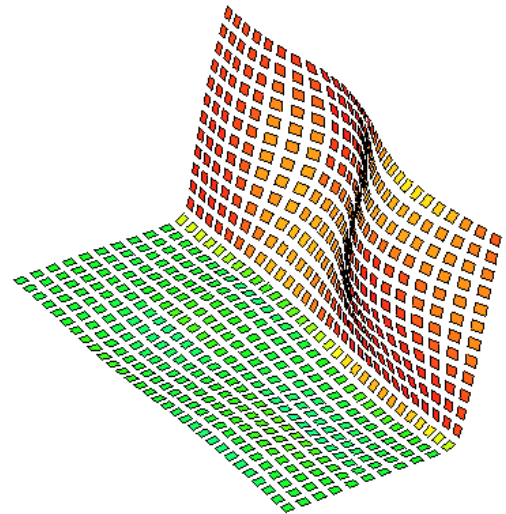


Figure 8 Geometry of the antenna array deformed by vibration mode 7 with resonance frequency of 229.62 Hz.

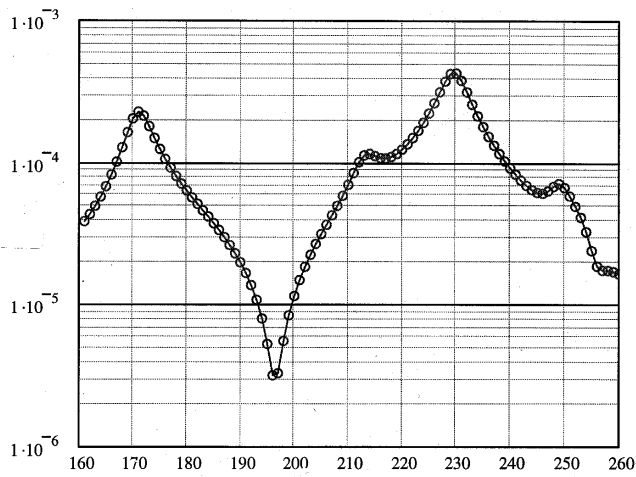


Figure 7 Frequency response function for front part of reconnaissance pod. On the vertical axis: Magnitude of FRF in m per m/sec.

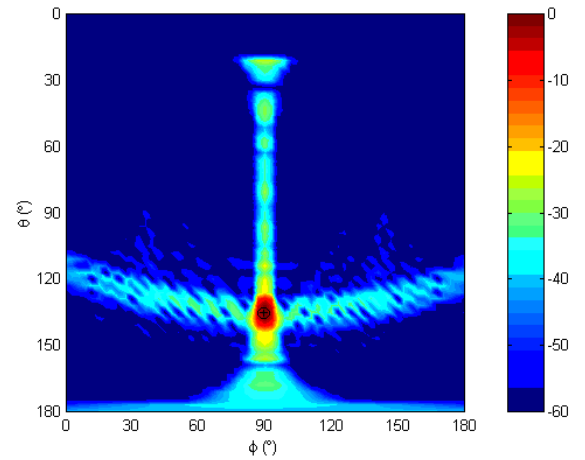


Figure 9 3-D radiation pattern of the non-deformed antenna array

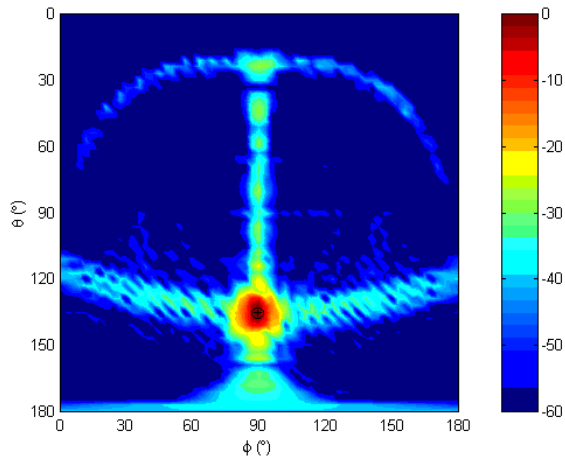


Figure 10 3-D radiation pattern of the antenna array, deformed by a vibration with resonance frequency of 229.62 Hz.

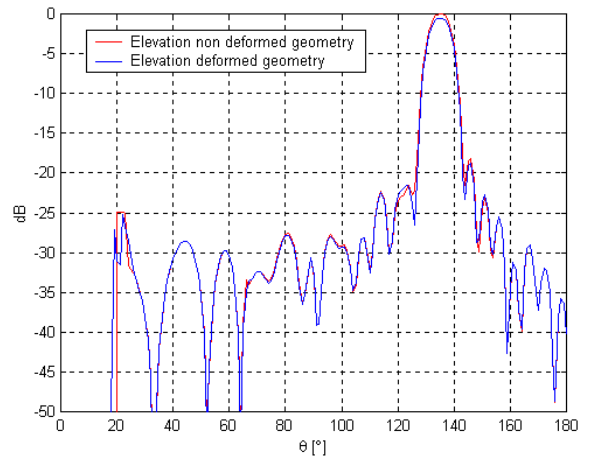


Figure 12 Elevation radiation pattern of the non-deformed antenna array versus the distorted pattern of the deformed array.

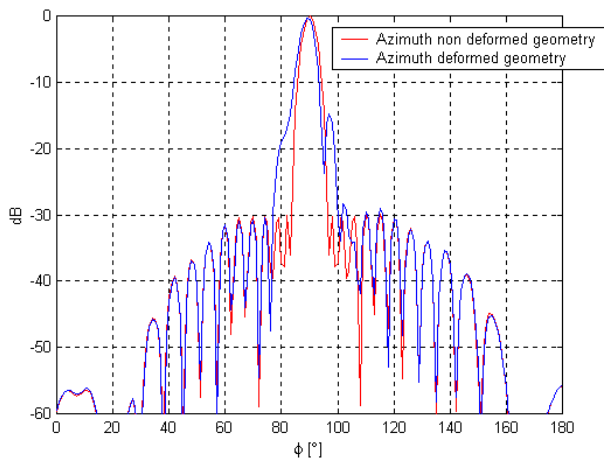


Figure 11 Azimuth radiation pattern of the non-deformed antenna array versus the distorted pattern of the deformed array.

